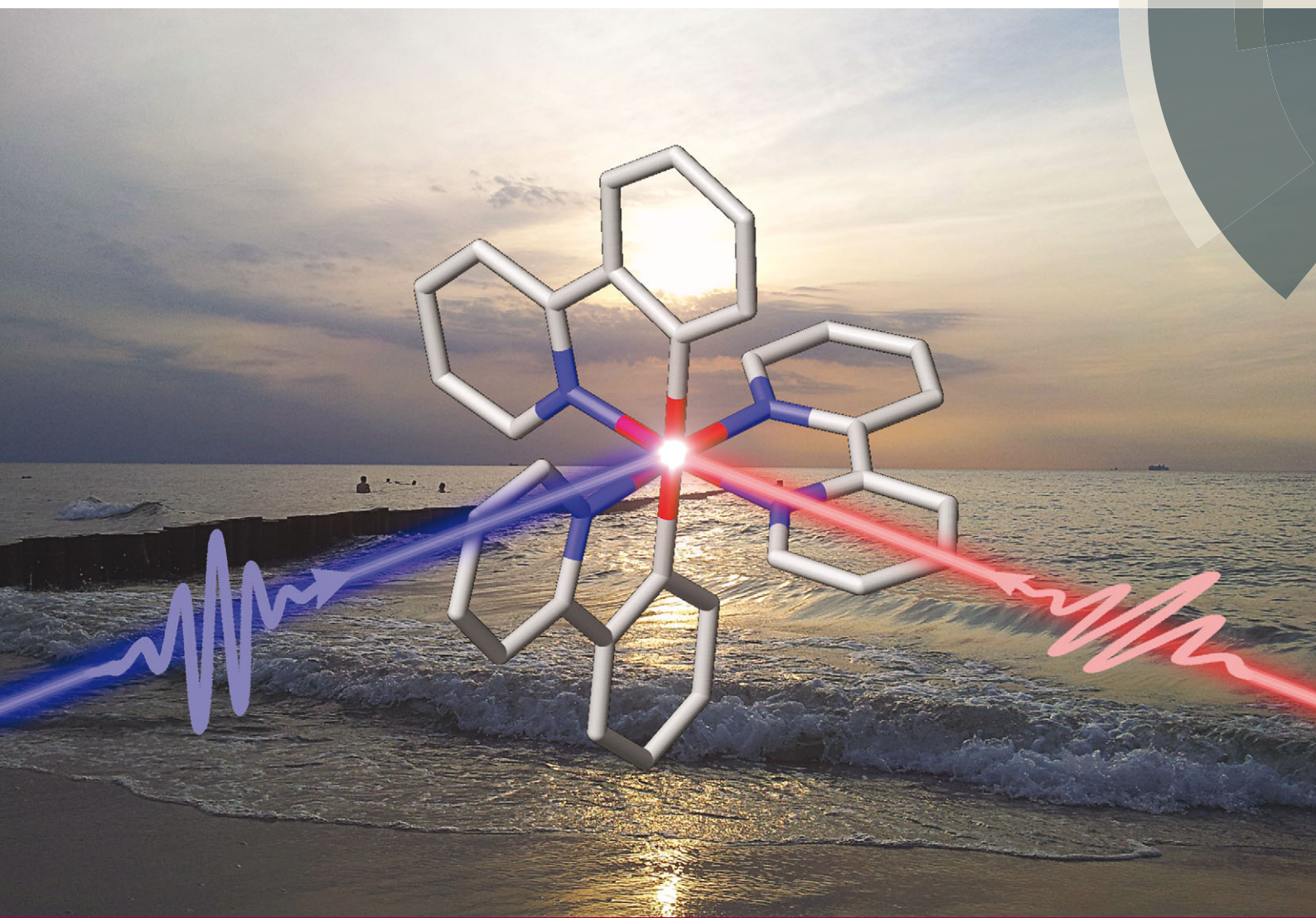


PCCP

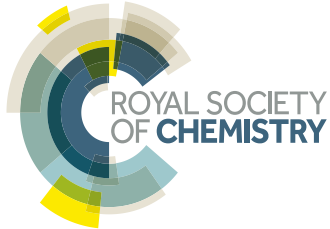
Physical Chemistry Chemical Physics

www.rsc.org/pccp



Themed issue: Bunsentagung 2016 - Basic Mechanisms in Energy Conversion

ISSN 1463-9076



COMMUNICATION

Stefanie Tschierlei, Stefan Lochbrunner *et al.*
Ultrafast excited state dynamics of iridium(III) complexes and their changes
upon immobilisation onto titanium dioxide layers

175 YEARS

COMMUNICATION

[View Article Online](#)
[View Journal](#) | [View Issue](#)

 Cite this: *Phys. Chem. Chem. Phys.*, 2016, 18, 10682

 Received 15th January 2016,
 Accepted 11th March 2016

DOI: 10.1039/c6cp00343e

www.rsc.org/pccp

Time-resolved spectroscopy was applied to investigate the excited state dynamics of two heteroleptic Ir(III) complexes with the general formula $[\text{Ir}(\text{C}^{\wedge}\text{N})_2(\text{N}^{\wedge}\text{N})]^+$, where $\text{C}^{\wedge}\text{N}$ and $\text{N}^{\wedge}\text{N}$ represent different cyclometalating and diimine ligands, respectively. The excited state relaxation is influenced by the ligand substitution as well as the light polarisation. Vibrational relaxation occurs in the sub-ps timescale and interligand charge transfer results in polarisation dependent signal dynamics with a time constant of about 30 ps. Electron injection from the iridium dye to TiO_2 is analysed with respect to potential applications in solar energy conversion.

Cyclometalated Ir(III) complexes¹ have been known for more than 30 years and their photophysical properties as well as excited state processes have been extensively studied since then, especially by Watts and coworkers.^{2,3} Their absorption, emission and electrochemical behaviour can be controlled by the exact choice of the ligands, which render them as ideal candidates for applications with respect to solar energy conversion and in photo(electro)chemical devices. Especially during the last decade cyclometalated Ir(III) complexes gained considerable scientific attention due to their usage in organic light emitting diodes,^{1,4} in light emitting electrochemical cells,^{5,6} as oxygen sensors^{7,8} and as photosensitisers for photocatalytic water splitting.^{9–18} In particular, their ability to generate hydrogen by the light-driven reduction of protons is still superior compared to Ru(II) polypyridine or Cu(I) bisdiimine complexes.^{15,19} Therefore, several systematic series of Ir(III) complexes with the general formula $[\text{Ir}(\text{C}^{\wedge}\text{N})_2(\text{N}^{\wedge}\text{N})]^+$, where $\text{C}^{\wedge}\text{N}$ is a monoanionic

cyclometalating ligand, have been prepared to broaden the scope of available sensitizers and to gain insight into the relationship between the structure and the resulting photophysical properties.^{1,5,6,17} In this regard, modifications were made to meet the following properties: (i) strong absorption in the visible region, (ii) long excited state lifetime, (iii) intense luminescence, (iv) electrochemical reversibility and (v) high stability under ambient conditions. As a result, highly luminescent Ir(III) complexes with quantum yields above 67% and emission lifetimes in the μs time range were prepared,¹⁵ which increased the probability of an electron-transfer process occurring prior to radiative or non-radiative relaxation. In-depth investigations of the underlying intermolecular reaction pathways of the iridium photosensitiser in the presence of a sacrificial electron donor such as triethylamine and an iron water reduction catalyst within a photocatalytic hydrogen evolving system revealed the different catalytic intermediates and the rate-limiting steps of the electron transfer processes.^{20–23} However, the initial light-induced intramolecular excited state processes in such $[\text{Ir}(\text{C}^{\wedge}\text{N})_2(\text{N}^{\wedge}\text{N})]^+$ complexes and their respective time constants are still not fully clarified. It is generally accepted that upon photoexcitation with visible light a transition into a singlet metal-to-ligand charge transfer (MLCT) state occurs. Subsequently, as a result of the iridium-induced strong spin-orbit coupling an ultrafast intersystem crossing (ISC) to the $^3\text{MLCT}$ state takes place within the first 100 fs,^{24–26} probably followed by vibrational relaxation to the respective lowest lying vibrational state in less than 700 fs.^{24,26–28} Furthermore, vibrational cooling involving energy transfer to the solvent^{25,26,29} or charge separation processes due to different types of surrounding ligands^{28,30} are found in the low picosecond time-range. However, the finally populated lowest lying triplet excited state, where the emission originates, is stable for several nano- or microseconds as required for photocatalytic applications.^{15,21,31,32}

In this work, time-resolved optical spectroscopy is used to study and compare the intramolecular relaxation dynamics of two different heteroleptic Ir(III) complexes, namely $[\text{Ir}(\text{ppy})_2(\text{bpy})]^+$ **1** and $[\text{Ir}(\text{ppy})_2(\text{bpy}(\text{COOH}))]^+$ **2** (ppy = monodeprotonated 2-phenylpyridine and bpy = 2,2'-bipyridine) (Fig. 1). While compound **1** often

^a Institute of Physics, University of Rostock, Albert-Einstein-Straße 23, 18059 Rostock, Germany. E-mail: stefan.lochbrunner@uni-rostock.de

^b Institute of Organic Chemistry, University of Stuttgart, Pfaffenwaldring 55, 70569 Stuttgart, Germany. E-mail: stefanie.tschierlei@oc.uni-stuttgart.de

^c Becker & Hickl GmbH, Nahmitzer Damm 30, 12277 Berlin, Germany

^d Leibniz-Institute for Catalysis at the University of Rostock (LIKAT), Albert-Einstein-Str. 29a, 18059 Rostock, Germany

† Electronic supplementary information (ESI) available: Experimental and synthetic details. UV-vis-, Raman- and time-resolved emission measurements. Transient absorption spectra of **1**, **2** and **2T**. See DOI: 10.1039/c6cp00343e

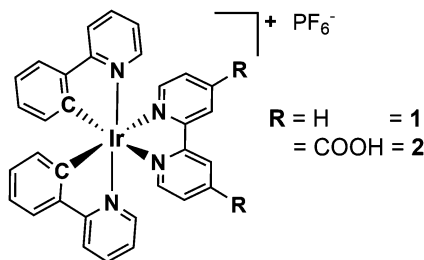


Fig. 1 Structure of the cyclometalated Ir(III) complexes **1** and **2** applied in this study.

serves as a reference complex for photophysical and photocatalytic studies, compound **2** bears two carboxyl anchor groups at the 4,4'-position in the bipyridine ligand for the immobilisation on semiconducting materials like TiO_2 or NiO .³³ This strategy of dye sensitisation is commonly used for the preparation of heterogeneous composite materials with the aim to broaden the light absorption of the semiconductor.^{33–35} Moreover, this immobilised system (abbreviated as **2T**) can be considered as a simple model of an anode of a dye-sensitised solar cell, where it is important to study the electron injection into the TiO_2 conduction band upon light irradiation.^{36,37}

Femtosecond time-resolved transient absorption spectroscopy addresses the intramolecular relaxation steps in **1** and **2** upon photoexcitation. Comparison of the behaviour of the two Ir(III) complexes discloses the influence of the carboxyl substituents and allows for conclusions on structure-dynamic-properties. Moreover, the effect of attaching **2** onto titania on the ultrafast excited state dynamics of **2** will be revealed and compared with the plain molecular system. Finally, this knowledge should contribute to the development of more efficient photosensitisers for applications in the field of solar energy conversion in the future.

Results and discussion

The Ir(III) complexes **1** and **2** were both synthesised and analysed according to literature procedures (Fig. 1).^{14,31,35,38} After purification **1** and **2** were obtained as yellow to orange solids with yields of 82% and 36%, respectively. The structures were confirmed by ^1H NMR spectroscopy and showed the typical pattern of the aromatic signals (ESI ‡). For the synthesis of **1** a slightly modified procedure was applied using ethanol as the only solvent. The iridium dimer $[(\text{ppy})_2\text{IrCl}]_2$ (ppy = monodeprotonated 2-phenyl-pyridine) and a slight excess of the bpy ligand were reacted in ethanol in a pressure tube at 100 °C for 2 days. Precipitation with excess of ammonium hexafluorophosphate and thoroughly washing with water and diethylether yielded the pure compound (ESI ‡). The complexes **1** and **2** possess a d^6 electron configuration and an octahedral structure (Fig. 1). Two more isomers, where either the ppy carbon atoms are *trans* to each other or one ppy carbon is *trans* to a ppy nitrogen and the other is *trans* to a bpy nitrogen, are not likely due to the stronger *trans* effect of Ir-C compared to Ir-N.¹

The absorption spectra of **1** and **2** (Fig. 2a and Fig. SI1, ESI ‡), which are similar to related cyclometalated Ir(III) complexes like

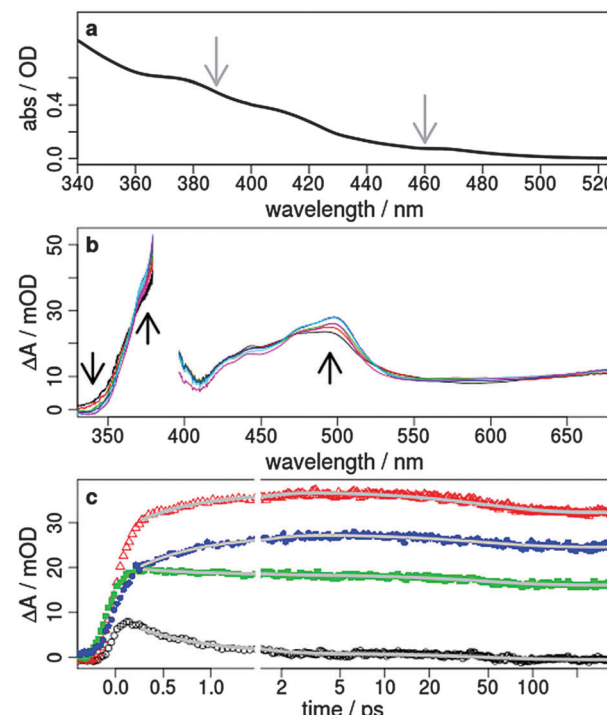


Fig. 2 (a) Steady-state absorption spectrum of **1** in acetonitrile. The excitation wavelengths of 388 and 460 nm for the time-resolved transient absorption studies are marked with grey arrows, (b) transient absorption spectra after 0.5, 0.8, 1.25, 2, 5 and 50 ps excited at 388 nm with laser pulses polarised perpendicular to the probe ($\text{mOD} = 10^{-3}$ optical density), and (c) transient signals as a function of the pump-probe delay time observed at 345 (black), 370 (red), 450 (green), and 500 nm (blue). The grey lines represent a double-exponential fit with the time constants $\tau_1 = 0.7$ ps and $\tau_2 = 48$ ps. The results of the decay associated spectra, comparison to other polarisations and transient spectra excited at 460 nm are summarised in the ESI ‡ .

the homoleptic analogue *fac*-[Ir(ppy)₃]³² exhibit the absorption bands of the spin-allowed $\pi-\pi^*$ transitions to the ppy and bpy ligand below 320 nm. In the visible region the absorption is assigned to spin-allowed metal-to-ligand charge transfer (MLCT) transitions ($\text{Ir}_d-\pi^*$) centred at about 390 and 420 nm.^{26,27,31,39} Furthermore, the very weak absorption above 460 nm is a contribution of the spin-forbidden singlet-to-triplet MLCT transitions as a consequence of the heavy-atom effect resulting in a strong spin-orbit coupling,³² which is also supported by theoretical calculations.^{40,41} A comparison of **1** and **2** reveals only a small impact of the carboxyl groups on the absorption properties.

In contrast, the emission (Fig. SI3, ESI ‡) is strongly influenced by the substituents resulting in different emission wavelengths and emission lifetimes. The emission maximum of **1** is located at 610 nm while it is red-shifted to 650 nm for **2** and the lifetime is decreased from 60.2 ± 0.4 ns (**1**) to 34.3 ± 0.2 ns (**2**). This behaviour is typical for the emission properties of similar Ir(III) or Ru(II) complexes with COOR substituents.^{31,42} Since the only structural difference between compound **2** and **1** is at the bpy ligand, it can be concluded that the lowest lying triplet excited state, from where the emission exclusively originates, corresponds to an MLCT state located at this ligand.

In order to analyse the relaxation dynamics of **1** and **2** in more detail, ultrafast time-resolved absorption measurements in acetonitrile solution were performed using 388 and 460 nm as pump wavelengths. These two wavelengths were selected, because they lie in the absorption band of the important MLCT transitions (Fig. 2a). Immediately after photoexcitation of **1** with 388 nm, a broad excited state absorption (ESA) appears in the visible region extending from 350 up to 700 nm, with two maxima at around 370 nm and 500 nm (Fig. 2b and ESI†). As apparent from the kinetics (Fig. 2c) the transient signals at 370 and 500 nm are increasing, while the bands at 340 and 440 nm decrease within the first 2 ps. For a quantitative evaluation the entire transient absorption change ΔA was globally analysed with the multi-exponential function $F(\lambda, t) = \sum_i^N c_i(\lambda) \cdot \exp(-t/\tau_i) + c_0$, with the probe wavelength λ , the delay time t and c_0 as a long-lived component.⁴³ It turns out that two exponential terms are needed for the description of the transient spectra. This global analysis of **1** resulted in a short time constant τ_1 of 700 fs and a longer one τ_2 of about 45 ps (Fig. 2 and Fig. SI4, SI5, ESI†; Table 1 and Table SI1, ESI†).

The fast component is associated with an absorption increase at around 370 and 500 nm and a decrease at 340 and 450 nm in the transient absorption spectra (Fig. 2). This is also confirmed by the negative and positive contributions of the fitted decay associated spectra (Fig. SI4, ESI†). The process is too slow for ISC in such Ir complexes and is more likely related to a subsequently occurring vibrational relaxation as also suggested by other groups.^{24,26–28} This assignment is further supported by the same observation for an excitation at 460 nm (Fig. SI5, ESI†), where the triplet MLCT states are directly populated.³² Moreover, such a vibrational relaxation does not change the dipole moment in **1**, resulting in the independency of this process on the polarisation of the light pulses. Thus, no differences could be found in the decay associated spectra for perpendicular and parallel polarised pump light at 388 and 460 nm (Fig. SI6, ESI†).

With respect to the second time constant τ_2 of about 45 ps (Table 1 and Table SI1, ESI†) the kinetics measured with parallel and perpendicular polarisations exhibit opposite trends (Fig. 3b and c, black rectangles). In the region between 350 and 530 nm the absorption increases for parallel polarised

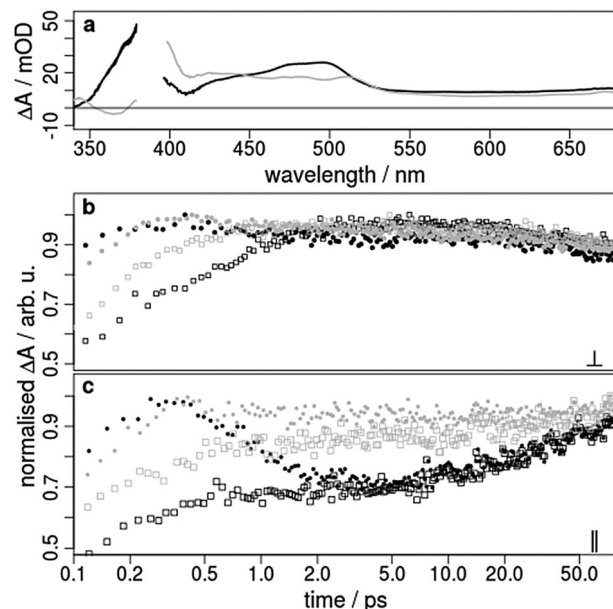


Fig. 3 Transient absorption spectra and kinetics of **1** (black) and **2** (grey) excited with 388 nm laser pulses. (a) Transient absorption spectra after 1 ps excited with perpendicular polarised light. (b) Transient signals as a function of the pump–probe delay time observed at 440 nm (points) and 500 nm (rectangles) excited with perpendicular polarised light. (c) as (b) but excited with parallel polarised light.

(Fig. 3c) and decreases somewhat with perpendicular polarised pump and probe pulses (Fig. 3b and Fig. SI4c, SI6, ESI†). This observation holds for both excitation wavelengths 388 nm and 460 nm. If the polarisations are set to magic angle, where both parallel and perpendicular parts of light are present, the contribution of the second exponential component is weak. These findings show that the second process must be associated with a change of orientation for the probed transition dipole. This cannot be explained by vibrational cooling processes or by interaction with the surrounding solvent molecules as suggested for other Ir(III) complexes.^{25,26,29} One possible explanation might be the occurrence of a light-induced interligand charge transfer (ILCT) process between ppy and bpy. This is in accordance with charge separation processes in slightly extended Ir(III) compounds^{28,30} and is comparable to interligand electron hopping in related coordination compounds such as Ru(II)^{44,45} Re(I)⁴⁶ and Os(II)⁴⁷ complexes. Therefore, we propose that after population of the two different triplet MLCT states of the ppy and bpy ligands an ILCT shifts the electron from the ppy onto the bpy ligand.

The observed transient absorption changes are dominated by dipole transitions of the reduced polypyridine ligands.²³ This is concluded from the fact that the ESA has a very similar shape compared to the absorption spectrum of the photochemically reduced Ir complex.²³ ILCT changes the transitions contributing to the ESA observed here. Since the ligands within the complex are almost perpendicularly oriented with respect to each other, the transition dipoles of the two interchanging ESA contributions are also more or less perpendicular. Accordingly, the electron transfer between the ligands changes the polarisation dependence of the ESA and causes the 30 ps dynamics. At the end, the final

Table 1 Summary of the time constants from the nonlinear least-square fitting of the transient kinetics and emission lifetimes of **1** and **2** in acetonitrile excited at 388 nm^a

Complex	Polarisation	τ_1 /ps	τ_2 /ps	τ_{em} ^b /ns
1	⊥	0.7	48	60.2
		0.7	43	
	ma	0.7	16	
2	⊥	0.3	17	34.3
		0.3	30	
	ma	0.3	16	

^a Under ambient oxygen concentration. ^b Excitation with unpolarised light.



relaxation of the excited states to the ground state is independent from the polarisation (Fig. SI6 top, ESI[†]) and takes place from the lowest lying triplet state located at the bpy ligand (see above).

Another reason for the 45 ps dynamics can be seen in the potential rotation of the molecule.⁴⁸ Calculation of the orientational relaxation time τ_{or} of **1** in acetonitrile results in approx. 52 ps (ESI[†]), which is on the same order of magnitude as that obtained in the experiment.

To evaluate the impact of substituents on the relaxation dynamics we studied complex **2** bearing two carboxyl anchor groups in 4,4'-position at the bpy ligand (Fig. 1). In the absorption spectrum of **2** the singlet MLCT band around 390 nm and the triplet MLCT absorption above 450 nm are somewhat more pronounced as in the spectrum of **1** (Fig. SI1, ESI[†]). This is probably an indication for an increased contribution of the substituted bpy ligand to the ground state absorption.⁴²

Also the transient spectra of both complexes **1** and **2** excited at 388 nm are very similar and show broad ESA in the visible region (Fig. 3a). The global data analysis of **2** yields two time constants ($\tau_1 = 0.3$ ps and $\tau_2 \approx 25$ ps), which are similar to those obtained for **1** (Table 1 and Table SI2, ESI[†]). Again τ_1 is independent of the applied polarisation (Fig. SI7 and SI8, ESI[†]), but this time τ_1 is slightly faster in **2** compared to **1**, showing the influence of the carboxy groups in the bpy ligand. Further, the time traces of **2** are not substantially influenced by the polarisation of the pump light as apparent from the comparison of the quite equal slope of the grey points in Fig. 3b and c at 440 and 500 nm. For the global analysis the second time constant τ_2 is solely necessary to fit kinetics below 420 nm as can be seen in the decay associated spectra (Fig. SI7, ESI[†]), which is in contrast to the analysis of **1**. Thus, population and depopulation of the excited states of **2** in the time period after 2 ps is probably negligible. This finding supports our assignment of τ_2 to an ILCT, because the triplet excited state of the substituted bpy ligand in **2** is lower in energy than the unsubstituted one. It seems that in **2** the electron is already promoted to the bpy ligand, and therefore, no ILCT is necessary to reach the lowest excited state (Fig. 5). Accordingly, the reorientation of the ESA dipole and the polarisation dependency is weak. These observations and conclusions also hold true for an excitation of **2** at 460 nm (Fig. SI8, ESI[†]).

Subsequently, the sensitisation of complex **2**, bearing two carboxylate anchor groups, on the TiO_2 @glass layer was performed by dip coating resulting in **2T** (ESI[†]). The successful immobilisation of **2** on the titania support was evidenced by UV/vis and Raman spectroscopy. It is found that the absorption of **2T** is a combination of the absorption spectrum of TiO_2 and of complex **2** (Fig. SI1, ESI[†]). Measurements of the non-resonant Raman spectra of **2** and **2T** show that the Raman bands of **2**, especially the modes of the ring stretching vibrations in the region between 1000 and 1650 cm^{-1} ,³⁹ could be also detected for the **2T** layer providing further evidence for the sensitisation of the TiO_2 surface by the dye (Fig. SI2, ESI[†]).

This sensitisation enables a photoinduced electron transfer from the iridium dye into the conduction band of the semiconductor.^{33,36,37} To obtain efficient injection a strong coupling

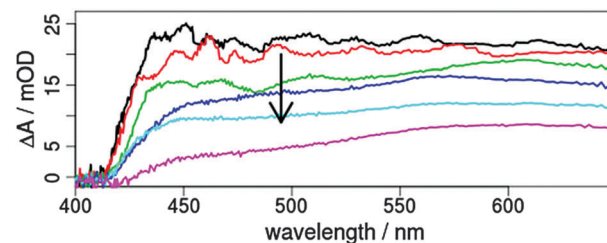


Fig. 4 Transient absorption spectra of the dye-sensitised TiO_2 -layer **2T** after 0.5 (black), 1 (red), 3 (green), 10 (blue), 50 (light blue) and 300 ps (magenta) excited at 388 nm with pulses perpendicular polarised to the probe. The observed changes are indicated with an arrow.

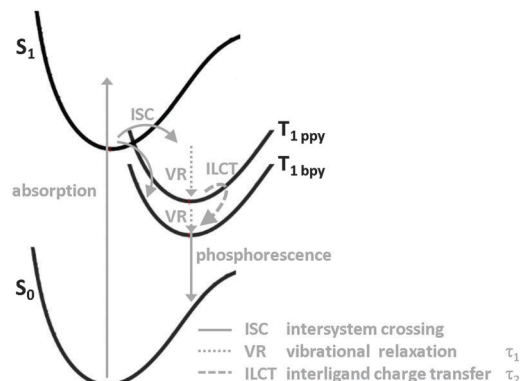


Fig. 5 Schematic representation of the relaxation processes in **1** and **2**. After light absorption and optical excitation of singlet metal-to-ligand charge transfer states involving the respective ppy and bpy ligands ISC to the triplet states occurs. This is followed by VR (τ_1) and ILCT (τ_2) between ppy and bpy, possibly accompanied by orientational relaxation of the molecule. Finally, phosphorescence (τ_{em}) from the triplet state takes place.

between the donor state of the dye and the acceptor state of titania is advantageous and the localisation of the excited MLCT state on the ligand with the anchoring substituents is beneficial. As shown for related Ru(II) complexes a transfer from singlet as well as triplet MLCT states can occur at sub-150 fs and tens of picoseconds, respectively.^{49,50} Further, time-resolved emission measurements for sensitised Ru(II) and Ir(III) complexes found multiexponential emission decays in about 500 ps.^{51,52} For **2T** the transient absorption shows a multi-exponential decay with time constants of 1.2, 13 and 150 ps (Fig. 4 and Fig. SI9, ESI[†]). In particular, the amplitudes of the short times are comparable to the results obtained for the lowest lying triplet excited state of **2** (Fig. SI7 and SI10, ESI[†]). This means that the triplet state is depopulated within 1.2 ps. The responsible process is most probably an electron transfer from the Ir complex to TiO_2 . In conclusion, the electron injection from the triplet MLCT localised at the bpy ligand to the conduction band of TiO_2 seems to be very efficient, which is a strong hint for successful sensitisation (either physical or chemical) of TiO_2 with **2**. In the future, time-resolved infrared spectroscopy may help to reveal the respective transfer steps in the titania to elucidate the nature of the three time constants in more detail.



Conclusions

In summary, we have prepared two iridium complexes **1** and **2** and successfully sensitised **2** onto a titania layer to form **2T**. A combination of absorption, emission and ultrafast time-resolved spectroscopy was used to elucidate the photophysical properties of these dyes (Fig. 5). The absorption spectra of both compounds are fairly similar. The presence of carboxyl substituents in **2** leads to a pronounced bathochromical shift (40 nm) of the emission maximum and a shorter emission lifetime. The triplet excited state, from where the emission originates, is located at the bpy ligand and is lower in energy for **2** compared to **1**.

After optical excitation and intersystem crossing vibrational relaxation occurs within 0.7 ps in **1** and is slightly faster in **2**, most likely due to the decreased energy of the bpy triplet MLCT state in **2**. In **1** an interligand charge transfer process from the ppy to the bpy ligand takes place within 45 ps and results in polarisation dependent transient spectra. The same process is inhibited in **2** due to the deeper level of the MLCT state involving the substituted bpy ligand. Investigation of **2T** revealed three time constants associated with electron injection. The fastest one (1.2 ps) can be ascribed to a transfer from the triplet state located at the bpy ligand to the conduction band of TiO_2 . However, the other two processes could not be assigned so far and are subject of further investigations.

In general, this study contributes to a better understanding of photoinduced energy and electron transfer processes that are crucial for solar energy conversion.

Acknowledgements

We thank Wolfram Seidel (University of Rostock) for the permission to use the Raman spectrometer. We gratefully acknowledge the state of Mecklenburg-Western Pomerania, the Federal Ministry of Education and Research of Germany (BMBF, project "Light2-Hydrogen") as well as the European Social Funds (ESF, "PS4H") for financial support. M. K. thanks the Fonds der Chemischen Industrie (FCI) for a fellowship.

Notes and references

- 1 L. Flamigni, A. Barbieri, C. Sabatini, B. Ventura and F. Barigelli, *Top. Curr. Chem.*, 2007, **281**, 143.
- 2 K. A. King, P. J. Spellane and R. J. Watts, *J. Am. Chem. Soc.*, 1985, **107**, 1431.
- 3 K. Dedeian, P. I. Djurovich, F. O. Garces, G. Carlson and R. J. Watts, *Inorg. Chem.*, 1991, **30**, 1685.
- 4 M. A. Baldo, M. E. Thompson and S. R. Forrest, *Nature*, 2000, **403**, 750.
- 5 C. Ulbricht, B. Beyer, C. Fribe, A. Winter and U. S. Schubert, *Adv. Mater.*, 2009, **21**, 4418.
- 6 R. D. Costa, E. Ortí, H. J. Bolink, F. Monti, G. Accorsi and N. Armaroli, *Angew. Chem., Int. Ed.*, 2012, **51**, 8178–8211.
- 7 K. K.-W. Lo, S. P.-Y. Li and K. Y. Zhang, *New J. Chem.*, 2011, **35**, 265.

- 8 X.-D. Wang and O. S. Wolfbeis, *Chem. Soc. Rev.*, 2014, **43**, 3666.
- 9 E. D. Cline, S. E. Adamson and S. Bernhard, *Inorg. Chem.*, 2008, **47**, 10378.
- 10 S. Jasimuddin, T. Yamada, K. Fukuju, J. Otsuki and K. Sakai, *Chem. Commun.*, 2010, **46**, 8466.
- 11 P. Zhang, P.-A. Jacques, M. Chavarot-Kerlidou, M. Wang, L. Sun, M. Fontecave and V. Artero, *Inorg. Chem.*, 2012, **51**, 2115.
- 12 H.-H. Cui, M.-Q. Hu, H.-M. Wen, G.-L. Chai, C.-B. Ma, H. Chen and C.-N. Chen, *Dalton Trans.*, 2012, **41**, 13899.
- 13 F. Gärtner, B. Sundararaju, A.-E. Sürküs, A. Boddien, B. Loges, H. Junge, P. Dixneuf and M. Beller, *Angew. Chem., Int. Ed.*, 2009, **48**, 9962.
- 14 F. Gärtner, D. Cozzula, S. Losse, A. Boddien, G. Anilkumar, H. Junge, T. Schulz, N. Marquet, A. Spannenberg, S. Gladiali and M. Beller, *Chem. – Eur. J.*, 2011, **17**, 6998.
- 15 F. Gärtner, S. Denurra, S. Losse, A. Neubauer, A. Boddien, A. Gopinathan, A. Spannenberg, H. Junge, S. Lochbrunner, M. Blug, S. Hoch, J. Busse, S. Gladiali and M. Beller, *Chem. – Eur. J.*, 2012, **18**, 3220.
- 16 D. R. Whang, K. Sakai and S. Y. Park, *Angew. Chem., Int. Ed.*, 2013, **52**, 11612.
- 17 A. Paul, N. Das, Y. Halpin, J. G. Vos and M. T. Pryce, *Dalton Trans.*, 2015, **44**, 10423.
- 18 C.-H. Tsai, D. N. Chirdon, H. N. Kagalwala, A. B. Maurer, A. Kaur, T. Pintauer, S. Bernhard and K. J. T. Noonan, *Chem. – Eur. J.*, 2015, **21**, 11517.
- 19 S.-P. Luo, E. Mejía, A. Friedrich, A. Pazidis, H. Junge, A.-E. Sürküs, R. Jackstell, S. Denurra, S. Gladiali, S. Lochbrunner and M. Beller, *Angew. Chem., Int. Ed.*, 2013, **52**, 419.
- 20 D. Hollmann, F. Gärtner, R. Ludwig, E. Barsch, H. Junge, M. Blug, S. Hoch, M. Beller and A. Brückner, *Angew. Chem., Int. Ed.*, 2011, **50**, 10246.
- 21 A. Neubauer, G. Grell, A. Friedrich, S. I. Bokarev, P. Schwarzbach, F. Gärtner, A.-E. Sürküs, H. Junge, M. Beller, O. Kühn and S. Lochbrunner, *J. Phys. Chem. Lett.*, 2014, **5**, 1355.
- 22 S. Fischer, O. S. Bokareva, E. Barsch, S. I. Bokarev, O. Kühn and R. Ludwig, *ChemCatChem*, 2016, **8**, 404.
- 23 S. I. Bokarev, D. Hollmann, A. Pazidis, A. Neubauer, J. Radnik, O. Kühn, S. Lochbrunner, H. Junge, M. Beller and A. Brückner, *Phys. Chem. Chem. Phys.*, 2014, **16**, 4789.
- 24 H.-S. Duan, P.-T. Chou, C.-C. Hsu, J.-Y. Hung and Y. Chi, *Inorg. Chem.*, 2009, **48**, 6501.
- 25 G. J. Hedley, A. Ruseckas and I. D. W. Samuel, *J. Phys. Chem. A*, 2009, **113**, 2.
- 26 G. J. Hedley, A. Ruseckas and I. D. W. Samuel, *J. Phys. Chem. A*, 2010, **114**, 8961.
- 27 F. Spaenig, J.-H. Olivier, V. Prusakova, P. Retailleau, R. Ziessel and F. N. Castellano, *Inorg. Chem.*, 2011, **50**, 10859–10871.
- 28 J. H. Klein, T. L. Sunderland, C. Kaufmann, M. Holzapfel, A. Schmiedel and C. Lambert, *Phys. Chem. Chem. Phys.*, 2013, **15**, 16024.
- 29 Y. You, K. S. Kim, T. K. Ahn, D. Kim and S. Y. Park, *J. Phys. Chem. C*, 2007, **111**, 4052.

30 C. Lambert, R. Wagener, J. H. Klein, G. Grelaud, M. Moos, A. Schmiedel, M. Holzapfel and T. Bruhn, *Chem. Commun.*, 2014, **50**, 11350.

31 J. B. Waern, C. Desmarests, L.-M. Chamoreau, H. Amouri, A. Barbieri, C. Sabatini, B. Ventura and F. Barigelli, *Inorg. Chem.*, 2008, **47**, 3340.

32 T. Hofbeck and H. Yersin, *Inorg. Chem.*, 2010, **49**, 9290–9299.

33 R. Marschall, *Top. Curr. Chem.*, 2016, **371**, 143.

34 M. Karnahl, E. Mejía, N. Rockstroh, S. Tschierlei, S.-P. Luo, K. Grabow, A. Kruth, V. Brüser, H. Junge, S. Lochbrunner and M. Beller, *ChemCatChem*, 2014, **6**, 82.

35 A. Kruth, S. Peglow, N. Rockstroh, H. Junge, V. Brüser and K.-D. Weltmann, *J. Photochem. Photobiol. A*, 2014, **290**, 31.

36 A. Hagfeldt, G. Boschloo, L. Sun, L. Kloo and H. Pettersson, *Chem. Rev.*, 2010, **110**, 6595.

37 A. Listorti, B. O'Regan and J. R. Durrant, *Chem. Mater.*, 2011, **23**, 3381.

38 M. S. Lowry, W. R. Hudson, R. A. Pascal and S. Bernhard, *J. Am. Chem. Soc.*, 2004, **126**, 14129.

39 S.-H. Lai, J.-W. Ling, Y.-M. Huang, M.-J. Huang, C. H. Cheng and I.-C. Chen, *J. Raman Spectrosc.*, 2011, **42**, 332.

40 S. I. Bokarev, O. S. Bokareva and O. Kühn, *J. Chem. Phys.*, 2012, **136**, 214305.

41 S. I. Bokarev, O. S. Bokareva and O. Kühn, *Coord. Chem. Rev.*, 2015, **304–305**, 133.

42 M. Schwalbe, M. Karnahl, S. Tschierlei, U. Uhlemann, M. Schmitt, B. Dietzek, J. Popp, R. Groake, J. G. Vos and S. Rau, *Dalton Trans.*, 2010, **39**, 2768.

43 S. Tschierlei, M. Karnahl, N. Rockstroh, H. Junge, M. Beller and S. Lochbrunner, *ChemPhysChem*, 2014, **15**, 3709.

44 S. Wallin, J. Davidsson, J. Modin and L. Hammarström, *J. Phys. Chem. A*, 2005, **109**, 4697.

45 S. Tschierlei, M. Presselt, C. Kuhnt, A. Yartsev, T. Pascher, V. Sundström, M. Karnahl, M. Schwalbe, B. Schäfer, S. Rau, M. Schmitt, B. Dietzek and J. Popp, *Chem. – Eur. J.*, 2009, **15**, 7678.

46 D. J. Liard, M. Busby, I. R. Farrell, P. Matousek, M. Towrie and A. Vlcek, *J. Phys. Chem. A*, 2004, **108**, 556.

47 G. B. Shaw, C. L. Brown and J. M. Papanikolas, *J. Phys. Chem. A*, 2002, **106**, 1483.

48 A. Henseler and E. Vauthey, *Chem. Phys. Lett.*, 1994, **228**, 66.

49 G. Benkő, J. Kallioinen, J. E. I. Korppi-Tommola, A. P. Yartsev and V. Sundström, *J. Am. Chem. Soc.*, 2002, **124**, 489.

50 J. Schindler, S. Kupfer, M. Wächtler, J. Guthmuller, S. Rau and B. Dietzek, *ChemPhysChem*, 2015, **16**, 1061.

51 E. I. Mayo, K. Kils, T. Tirrell, P. I. Djurovich, A. Tamayo, M. E. Thompson, N. S. Lewis and H. B. Gray, *Photochem. Photobiol. Sci.*, 2006, **5**, 871.

52 Y. Tachibana, I. V. Rubtsov, I. Montanari, K. Yoshihara, D. R. Klug and J. R. Durrant, *J. Photochem. Photobiol. A*, 2001, **142**, 215.

